View metadata, citation and similar papers at core.ac.uk

brought to you by CORE

provided by DSpace at VU

JOURNAL OF VIROLOGY, Nov. 2005, p. 13326–13337 Vol. 79, No. 21
0022-538X/05/$08.00+0 doi:10.1128/JVI.79.21.13326–13337.2005
Copyright © 2005, American Society for Microbiology. All Rights Reserved.

In Nasopharyngeal Carcinoma Cells, Epstein-Barr Virus LMP1 Interacts with Galectin 9 in Membrane Raft Elements Resistant to Simvastatin

Catherine Pioche-Durieu,[1]† Cécile Keryer,[1]† Sylvie Souquère,[2] Jacques Bosq,[3] Wolfgang Faigle,[4] Damarys Loew,[4] Mitsuomi Hirashima,[5] Nozomu Nishi,[6] Jaap Middeldorp,[7] and Pierre Busson[1]*

UMR 8126 CNRS, Institut Gustave Roussy, Villejuif, France[1]; CNRS UPR 1983, Institut André Lwoff, Villejuif, France[2]; Département d'Anatomie Pathologique, Institut Gustave Roussy, Villejuif, France[3]; Laboratoire de Spectrométrie de Masse, Institut Curie, 75005 Paris, France[4]; Department of Immunopathology, Faculty of Medicine, Kagawa University, Japan[5]; Department of Endocrinology, Faculty of Medicine, Kagawa University, Japan[6]; and Department of Pathology, Free University Hospital, De Boelelaan 1117, 1081 HV Amsterdam, The Netherlands[7]

Received 1 May 2005/Accepted 22 July 2005

Nasopharyngeal carcinomas (NPC) are etiologically related to the Epstein-Barr virus (EBV), and malignant NPC cells have consistent although heterogeneous expression of the EBV latent membrane protein 1 (LMP1). LMP1 trafficking and signaling require its incorporation into membrane rafts. Conversely, raft environment is likely to modulate LMP1 activity. In order to investigate NPC-specific raft partners of LMP1, rafts derived from the C15 NPC xenograft were submitted to preparative immunoprecipitation of LMP1 combined with mass spectrometry analysis of coimmunoprecipitated proteins. Through this procedure, galectin 9, a beta-galactoside binding lectin and Hodgkin tumor antigen, was identified as a novel LMP1 partner. LMP1 interaction with galectin 9 was confirmed by coimmunoprecipitation and Western blotting in whole-cell extracts of NPC and EBV-transformed B cells (lymphoblastoid cell lines [LCLs]). Using mutant proteins expressed in HeLa cells, LMP1 was shown to bind galectin 9 in a TRAF3-independent manner. Galectin 9 is abundant in NPC biopsies as well as in LCLs, whereas it is absent in Burkitt lymphoma cells. In subsequent experiments, NPC cells were treated with Simvastatin, a drug reported to dissociate LMP1 from membrane rafts in EBV-transformed B cells. We found no significant effects of Simvastatin on the distribution of LMP1 and galectin 9 in NPC cell rafts. However, Simvastatin was highly cytotoxic for NPC cells, regardless of the presence or absence of LMP1. This suggests that Simvastatin is a potentially useful agent for the treatment of NPCs although it has distinct mechanisms of action in NPC and LCL cells.

Nasopharyngeal carcinoma (NPC) is one of the best examples of a human solid tumor which is consistently associated with a virus (7). NPC is rare in Europe and North America (<3 cases/100,000 persons/year), but it remains a major public health problem in several areas of Asia and Africa. Very-high-incidence foci are found in south China, especially in Guandong and Guangxi provinces (25 to 40 cases per 100,000 persons per year) and also in other populations of southeast Asia, for example, in the Sarawak people of Borneo island (14). Intermediate risk areas include the Philippines, Vietnam, Indonesia, and several countries of North and West Africa (incidence of 4 to 8 cases/100,000 persons/year). Most NPCs have minimal epithelial maturation and are classified as undifferentiated (World Health Organization [WHO] type III) or poorly differentiated (WHO type II). A few cases are differentiated (WHO type I). Epstein-Barr virus (EBV) association is constant regardless of patient origin and tumor differentiation except for some very rare cases of differentiated NPC (type I) in western countries (47). Another striking constant feature of NPC is the presence of a massive lymphoid infiltrate in the primary tumor. This infiltrate contains mostly T lymphocytes and a minority of B cells, monocytes, eosinophils, and dendritic cells. It results at least in part from a massive production of inflammatory cytokines by malignant cells, including interleukin 1α, interleukin 1β and macrophage inhibitory protein 1 (6, 26, 57).

EBV infection in NPC cells is mainly latent. Several copies of the EBV genome (about 170 kb) are contained in the nuclei of malignant cells, generally in the form of circular independent DNA molecules called episomes. Most of the about 80 EBV genes are silent in NPC cells, but some of them are consistently expressed (50). Two of these genes encode small untranslated EBV-encoded RNAs (28). Other EBV genes consistently transcribed in NPC encode viral proteins with proven or suspected oncogenic properties like Epstein-Barr nuclear antigen 1 (EBNA1), latent membrane protein 1 (LMP1) and LMP2, and the BARF1 protein (5, 23, 55). Currently, only EBNA1 and LMP1 are detected in NPC cells by routine immunohistochemistry (detection of LMP2 requires special techniques to enhance antibody staining) (23). EBNA1 is a chromatin-associated protein that is involved in EBV genome

* Corresponding author. Mailing address: Institut Gustave Roussy, CNRS UMR 8126, Villejuif Cedex 94805, France. Phone: 33 1 42 11 45 83. Fax: 33 1 42 11 54 94. E-mail: pbusson@igr.fr.

† C.P.-D. and C.K. contributed equally to this work.

maintenance and is also suspected to have an oncogenic role (34). LMP1, which is regarded as the main EBV oncoprotein, is a membrane-associated protein trafficking in the internal and plasma membranes. Its role in NPC oncogenesis has been questioned because its expression is heterogenous, variable from one biopsy to another and within a given specimen (16) (36). However, extensive sequence analysis of EBV tumor isolates reveals frequent invalidation of LMP1 T-cell epitopes and strongly suggests that it is expressed in NPC cells despite a negative pressure of the immune system (17). This observation supports the notion that LMP1 has a role in the malignant phenotype of NPC cells. In addition, we have found that LMP1 expression is more consistent and abundant in the juvenile form of North African NPCs, which differs from the adult form by several clinical and biological characteristics (35, 36).

LMP1 is a 386-amino-acid protein with a short N-terminal intracytoplasmic domain (24 residues), six transmembrane segments joined by short internal and external loops, and a long C-terminal intracytoplasmic domain (190 residues). The N-terminal domain and the transmembrane segments have a key role in membrane anchoring, intracellular trafficking, and self-aggregation of the protein (19, 29, 65). On the other hand, the C-terminal intracytoplasmic domain can bind a series of cellular signaling adaptors including TRAF3, tumor necrosis factor receptor-associated death domain (TRADD) protein, and the gp85 subunit of the phosphatidylinositol 3-kinase (46), (37), (13). There is a suspicion that the N terminus and transmembrane portions can also bind signaling adaptors, but so far none has been formally identified (33, 49, 65). LMP1 has the ability to activate a wide range of signaling pathways. The assortment of these pathways and the resulting effects are dependent on the context of the host cell, the nature of LMP1 strain polymorphisms, and LMP1 cellular concentration (18, 27, 39, 45, 66). In EBV-transformed B cells, LMP1 signaling pathways are adjusted in order to draw cells through the G_1/S checkpoint and simultaneously prevent apoptosis in a majority of cells (15). There is a consensus that three types of molecular processes are required for optimal activation of most LMP1 signaling pathways: its own oligomerization; the capture of its signaling adaptors, especially TRAF3, TRAF6, and TRADD; and its incorporation into membrane rafts (19, 32, 43, 64). Membrane rafts are microdomains of the cell membrane network characterized by a high content in cholesterol and glycosphingolipids. These microdomains are sites of preferential attachment for glycosylphosphatidylinisitol-anchored (external membrane layer) and nonreceptor tyrosine kinases (internal membrane layer). Most raft components are recovered as buoyant complexes through a procedure of cell fractionation and flotation on a density gradient. Most authors simply identify membrane rafts to buoyant complexes, as we will do ourselves in the rest of this report. However, one needs to keep in mind that there are several categories of rafts that are not discriminated by flotation assays although they have distinct content in situ (48). The exact nature of the raft-like complexes carrying LMP1 has remained elusive since we first reported the association of LMP1 with these subcellular elements (11). Although we along with others have shown that LMP1 recruits its main signaling adaptor TRAF3 in raft-like complexes, so far we have not been able to identify additional cellular partners of LMP1 in these structures (1, 2, 24, 32, 65). Kaykas et al. (32) have reported that artificial targeting of the LMP1 C-terminal domain to classical membrane rafts only partially restores its signaling activity. As noted by these authors, there is something "special" in natural rafts carrying LMP1 that is required for its maximal signaling ability.

In order to progress in the characterization of these complexes, we undertake to identify novel partner proteins associated with LMP1 in membrane rafts using a direct approach based on preparative immunoprecipitation and mass spectrometry (MS) analysis. This approach was applied to NPC cells having spontaneous LMP1 expression. We report that LMP1 interacts with galectin 9, a protein previously identified in Hodgkin's disease, which appears to be extremely abundant in NPC cells. Association of LMP1 and galectin 9 with the rafts was not inhibited by the raft-modifying agent Simvastatin, in contrast with a previous report regarding EBV-transformed B cells (31). However, Simvastatin appeared to be highly cytotoxic for NPC cells by an LMP1-independent mechanism.

MATERIALS AND METHODS

Tumor and cell lines. C15 and C17 are EBV-positive NPC tumor lines permanently propagated by subcutaneous passage into nude mice (6). C666-1 is an EBV-positive NPC cell line which can be propagated by in vitro culture (9). It was kindly provided by D. P. Huang and K. W. Lo (Chinese University of Hong Kong). C15 cells consistently produces LMP1, whereas LMP1 production is undetectable at the protein level in C17 and C666-1 cells (9, 11). Non-NPC malignant epithelial cell lines were also used: HeLa (cervix carcinoma), A431 (vulvar epidermoid carcinoma), and HT 29 and HCT 116 (both colonic carcinomas). EBV1 and NAD+C15 are lymphoblastoid cell lines (LCL) resulting from EBV transformation of normal B lymphocytes and are infected with the B95-8 and the C15 strain of EBV, respectively (1). Several Burkitt lymphoma cell lines were used: Ramos (EBV negative), BL2 (EBV negative), and Daudi (EBV positive without endogenous LMP1 expression). BL2-B95 resulted from the conversion of BL2 by the B95-8 strain of EBV. Daudi-LMP6 is a subclone of Daudi transfected with the B95-8 LMP1 gene under the control of the human metallothionein promoter (63).

Eukaryotic expression vectors and transfections. All transfected genes were expressed by short-term transfections, except for the previously described HL8 clone derived from HeLa cells and having stable expression of the full-length B95-8 LMP1 under the control of the metallothionein promoter (2). Short-term transfections were also done in HeLa cells using DOTAP (*N*-[1-(2,3-dioleoyloxy)propyl]-*N*,*N*,*N*-trimethylammonium methylsulfate) cationic liposomes (Roche Molecular, Meylan, France). Cells were harvested 24 h after transfection. The full-length galectin 9 cDNA encoding the shortest isoform lacking exons 5 and 10 was expressed under the control of the cytomegalovirus (CMV) promoter in the pBK-CMV plasmid from Stratagene (La Jolla, CA). LMP1 cDNA from the B95-8 strain, either full-length or deleted of the PXQXT motif at codons 204 to 208, was expressed from the pcDNA3 plasmid (Invitrogen) (2).

Antibodies. LMP1 was detected using three types of reagents. CS1-4 (Dako-Cytomation, Denmark) is a pool of four monoclonal antibodies directed to the C terminus of LMP1; its target epitopes map in the variable 11 amino acid repeats between residues 205 to 308 and close to residue 386 at the very C terminus (44, 52). CS1-4 was used under the form of hybridoma culture supernatant, as provided by the manufacturer. OT21C is a monoclonal antibody that reacts with a conformational epitope mapping at residues 290 to 318, thus overlapping the 11 amino acid repeats of LMP1 (44). OT21C was affinity purified and used mainly for immunoprecipitation. OT22CN is a monoclonal antibody that reacts with an epitope contained in residues 1 to 23 in the amino-terminal intracytoplasmic portion of LMP1 (44). It was also affinity purified prior to its use in this study. Galectin 9 was detected using an affinity-purified polyclonal antibody raised against the C-terminal carbohydrate recognition domain of human galectin 9, whose central motif maps at residues 287 to 293. Affinity-purified antibodies against TRAF3 (H122), Lyn (clone 42), poly(ADP-ribose) polymerase (PARP; clone C-2-10) and CD40 (monoclonal antibody [MAb] 89) were from Santa Cruz (Heidelberg, Germany), Transduction Laboratories (Becton Dickinson, Le Pont de Claix, France), Merck Biosciences (Darmstadt, Germany), and Beckman Coulter (Villepinte, France), respectively. The anti-CD40 antibody G28-5 was produced using the corresponding hybridoma

(American Type Culture Collection; clone HB 9110) and purified by protein A chromatography.

Whole-tumor or cultured cell protein extraction. Small tumor pieces were transferred in a small volume of RIPA buffer (150 mM NaCl, 25 mM Tris-HCl, pH 7.5, 5 mM EDTA, 0.5% sodium deoxycholate, 0.5% NP 40, 0.1% sodium dodecyl sulfate [SDS]) supplemented with Complete protease inhibition mixture according to the manufacturer's instructions (Roche Molecular, Meylan, France). Tumor pieces were homogenized in a tight-fitting conical glass homogenizer and sonicated (three times for 10 s each time) on ice. Extracts were clarified by centrifugation for 15 min at 16,000 × *g* at 4°C. Cultured cells were simply solubilized in RIPA buffer with Complete protease inhibition mixture, sonicated, and clarified in the same way as for tumor extracts.

Isolation of rafts (flotation assay). Rafts were isolated by Triton X-100 extraction and flotation through a sucrose step gradient as previously described (1, 2, 11). Briefly, tumor pieces (500 mg) or cell suspensions (about 10^8 cells) were homogenized at 4°C in 3 ml of MES (morpholineethanesulfonic acid)-buffered saline (MBS) containing 1% Triton X-100 and the protease inhibition mixture (Complete). A 100-μl aliquot of this unfractionated extract was saved for Western blot analysis (designated initial extract). The remainder was clarified by centrifugation at 50 × *g* for 2 min. The pellet was collected and named LSP (low speed pellet). The clarified homogenate was made up to 4 ml in 1.2 M (40%) sucrose–MBS–Triton at 4°C, transferred to an SW41 ultracentrifuge tube, and overlaid with 4.5 ml of 0.9 M (30%) sucrose-MBS buffer (without Triton) and a third layer of 2.7 ml of MBS (without sucrose). This step gradient was centrifuged at 180,000 × *g* at 4°C in an SW41 Ti Beckman rotor for 18 to 20 h. The raft fraction, visible as an opaque band 5 mm below the interface of the upper and middle gradient layers, was harvested. The sample was diluted to a final volume of 3 ml in MBS and pelleted in a TLA 100.3 Beckman rotor (300,000 × *g* at 4°C for 60 min). The amount of proteins in the upper and the 30% sucrose layers were consistently negligible. The 40% sucrose layer was collected and named fraction F40. Finally, a pellet of heavy Triton-insoluble material was retained and named fraction HSP (high speed pellet). For protein assays and Western blot analysis, the LSP, HSP, and raft pellets were solubilized in approximately 10 volumes of RIPA buffer supplemented with SDS (6% final concentration). Similarly, aliquots of the unfractionated lysate and the F40 fractions were further diluted and homogenized in 6% SDS-RIPA buffer. Rafts were used for preparative or analytical immunoprecipitations. In other experiments, all fractions—initial extract, LSP, HSP, rafts, and F40—were analyzed by direct polyacrylamide gel electrophoresis (PAGE) and Western blotting. The relative concentration of various protein species in the rafts by comparison with the initial extract was estimated by the ratio of the densitometric "volumes" (V) of the corresponding bands: V raft/V initial.

Protein concentration assay. In all tumor and cell extracts or fractions, protein concentration was assayed by the Lowry method using a detergent-compatible microassay system (Bio-Rad, Marnes-la-Coquette, France).

Western blotting. Western blotting was performed on polyvinylidene difluoride membranes (Immobilon P; Millipore, St. Quentin en Yvelines, France) according to standard protocols, using horseradish peroxidase-conjugated secondary antibodies and the ECL system (Amersham, Les Ulis, France). In one instance (see Fig. 2c), a Supersignal Westfemto kit (Pierce, Brebières, France) was used for revelation of horseradish peroxidase-conjugated secondary antibodies instead of the ECL system. For a given PAGE gel, the amounts of total proteins loaded in each lane were identical (for example, 30 μg). When required, densitometry of the chemiluminescence films was done using a GS-710 calibrated imaging densitometer with Quantity One software (Bio-Rad, Marnes-la-Coquette, France).

Immunoprecipitations. Affinity-purified antibodies were loaded on magnetic beads according to the manufacturer's instructions (Dynal Biotech ASA, Compiègne, France). Pan-mouse immunoglobulin G (IgG) or protein A Dynabeads were used for murine monoclonal or rabbit polyclonal antibodies, respectively. For some experiments, antibodies were covalently cross-linked on magnetic beads using DMP (dimethyl pimelimidate dihydrochloride) according to the manufacturer's instructions (Dynal Biotech).

(i) Preparative immunoprecipitations. Preparative immunoprecipitations were made on raft complexes prior to tandem MS (MS/MS) analysis, using 45 μg of OT21C monoclonal antibody covalently cross-linked on 4.5×10^8 pan-mouse IgG Dynabeads. Purified mouse IgG1 was used for some of the negative controls (Sigma). Antigen capture was performed by overnight incubation of 4.5×10^8 IgG-loaded beads with a raft sample corresponding to 180 μg of protein diluted in 1.8 ml of immunoprecipitation buffer (10 mM Tris-HCl, pH 7.4, 150 mM NaCl, 1% Triton X-100). Magnetic beads carrying the immune complexes were subsequently washed six times in washing buffer (10 mM Tris-HCl, pH 7.4, NaCl 150 mM, 1% Triton X-100, 60 mM octyl β-D-glucopyranoside). Precipitated proteins were eluted by boiling the beads for 5 min in 120 μl of a modified form of Laemmli buffer with a high content of SDS (50 mM Tris, 75 mM NaCl, 2.5 mM EDTA, 10% glycerol, 5% SDS). A small aliquot of eluted proteins (6 μl) was saved for quality controls of the immunoprecipitation step based on Western blot detection of LMP1 and TRAF3. The rest was further processed for MS analysis.

(ii) Analytical immunoprecipitations. Analytical immunoprecipitations were done using the same basic procedure, with some modifications according to the type of precipitating antibodies and the type of tumor or cell extract. Analytical immunoprecipitations were made on the rafts with anti-LMP1 monoclonal antibodies using the above-mentioned conditions, except that only 5 μg of antibodies was loaded on 5×10^7 beads in order to save reagents (without covalent cross-linking unless otherwise mentioned). Loaded beads were then incubated with a raft sample containing 60 μg of protein diluted in 600 μl of immunoprecipitation buffer (unless otherwise mentioned). Eluted proteins were analyzed by Western blotting. The same procedure was carried out for immunoprecipitation on whole-tumor extracts except for two points: loaded beads were incubated with a sample of tumor extract containing 120 μg of protein in 600 μl of immunoprecipitation buffer, and protease inhibition mixture (Complete) was added to the immunoprecipitation buffer. For direct immunoprecipitation of galectin 9, an affinity-purified polyclonal antibody was bound to protein A Dynabeads at a ratio of 10 μg to 80 μl of beads. Rabbit nonspecific purified immunoglobulins were used for the control experiments (Sigma). Antigen capture was performed by a 4-h incubation of 20 μl of Ig-loaded beads with a raft sample corresponding to 30 μg of protein or 30 μl of loaded beads with 120 μg of whole-cell extract.

MS analysis of proteins coimmunoprecipitated with LMP1. (i) SDS-PAGE separation and protein digestion. Precipitated proteins eluted from beads were loaded in a 5% SDS-PAGE gel for a short migration (about 1 cm) in order to remove detergents incompatible with MS analysis and further reduce the complexity of the eluted samples. Unstained segments of gel lanes containing proteins were cut in nine slices (width, about 1 mm) from low to high molecular weights. Each slice was treated as a distinct source of protein digests. Practically, slices were cut in 1- by 1-mm pieces which were washed three times by sequential immersions in 25 mM $NH_4 \cdot HCO_3$ and plain acetonitrile and then dried. Dried gel pieces were reduced and alkylated by using dithiothreitol and iodoacetamid, respectively. Gel pieces were dried again after a new cycle of washes as described above. In-gel trypsin digestion was performed overnight at 30°C (20 ng/μl in $NH_4 \cdot HCO_3$ solution; Sigma). Finally, protein digests were extracted by the addition to gel pieces of a mixture of acetonitrile–H_2O–HCOOH (60:35:5 [vol/vol/vol]), followed by sonication and centrifugation. Supernatants containing tryptic peptides were vacuum dried to a very small volume (1 or 2 μl) and then diluted again in 5% acetonitrile (H_2O, 95%).

(ii) Liquid chromatography and MS/MS analysis. Concentrated peptides were separated on an LC Packings system (Dionex) coupled to the nanoelectrospray II ionization interface of a QSTAR/Pulsar I (Applied Biosystems). The MS/MS data from the different experiments were analyzed using MASCOT software on an internal server (Matrix Science, London, United Kingdom). The protein search was done in three rounds, one without taxonomic restrictions, one against the NCBI human database, and one against the murine database.

Confocal immunofluorescence analysis. Cells were fixed on poly-L-lysine slides at room temperature using 4% paraformaldehyde for 15 min, permeabilized in 0.1% SDS in phosphate-buffered saline (PBS) for 10 min, and then incubated for 20 min with 10% FCS–0.2% bovine serum albumin–PBS for saturation of nonspecific binding sites. Antibodies were diluted in PBS–0.2% bovine serum albumin. The mouse monoclonal OT22CN directed to the N-terminal domain of LMP1 was diluted to 2 μg/ml. The rabbit polyclonal antibody against galectin 9 was the same as for Western blotting, used at 5 μg/ml. Secondary anti-mouse and anti-rabbit antibodies were conjugated to Alexa 546 and Alexa 488, respectively (Molecular Probes, Invitrogen, Cergy-Pontoise, France). Observations were made with a confocal microscope (Zeiss LSM510).

Immunostaining of fresh NPC biopsies. Tissue sections were dewaxed, rehydrated, and microwaved at 98°C for 20 min in citrate buffer (10 mM, pH 7.3). After endogenous peroxidase was blocked with H_2O_2, they were incubated with the affinity-purified anti-galectin 9 rabbit antibody at 5 μg/ml for 60 min at room temperature. In the next step, sections were incubated with the EnVision polymer (DakoCytomation, Trappes, France) conjugated to peroxidase for 45 min at room temperature and subsequently with diaminobenzidine used as a chromogenic substrate of peroxidase. Finally, sections were counterstained with Mayer's hematoxylin for 8 s, dehydrated, and mounted.

Electron microscopy. Cell pellets were fixed with 1.6% glutaraldehyde at 4°C, followed by treatment with osmium tetroxide, and then dehydrated and embedded in Epon resin. Ultrathin sections were cut on an LKB-III ultra-microtome, stained for contrast with uranyl acetate and lead citrate, and examined with a Zeiss EM 902 transmission electron microscope.

FIG. 1. Assessment of preparative LMP1 immunoprecipitation from C15 rafts using the OT21C antibody. Samples of C15 rafts corresponding to 60 μg of protein were submitted to immunoprecipitation using 15 μg of purified OT21C or irrelevant mouse IgG1 covalently bound to 1.5×10^8 magnetic beads. Parallel blots were stained with anti-LMP1 (CS1-4), anti-TRAF3, and anti-Lyn. The last blot was restained with β-actin antibodies. Input, raft-derived proteins saved prior to the immunoprecipitation step (5 μg, LMP1; 10 μg, TRAF3, Lyn, and β-actin); mIgG1, one-third of the eluted proteins recovered from control immunoprecipitation (irrelevant mouse IgG1); OT21C, one-third of the eluted proteins recovered from LMP1 immunoprecipitation. Using the above-mentioned ratios of magnetic beads, antibodies, and raft proteins, about 100% of LMP1 and 50% of TRAF3 were recovered by immunoprecipitation with OT21C. All the experiments depicted in this and subsequent figures were performed at least twice.

In vitro pharmacological assays on NPC cells. Prior to in vitro experiments, xenografted C15 tumors were minced and treated with type II collagenase for cell dispersion as previously described (54). Residual cell aggregates were removed by filtration on a nylon cell strainer with 100-μm pores. C15 cell suspensions were grown in HEPES-buffered RPMI medium with 7.5% fetal calf serum on plastic coated with poly(2-hydroxyethylmethacrylate) (polyHEMA; Sigma, Saint-Quentin Fallavier, France), an antiadhesive polymer that inhibits cell attachment (60). Using this coating procedure, proliferation of murine fibroblasts was completely inhibited, whereas NPC cells grew as nonanchored spheroids or aggregates about 150 μm in diameter. Preactivated Simvastatin was solubilized in dimethylsulfoxide (DMSO; 10 mM stock solution) (Calbiochem/Merck). For biochemical experiments, C15 cells were seeded in 24-well plates at 1 million cells/well in 1.5 ml of culture medium and incubated with Simvastatin for 5 days at a final concentration of 5 μM. Control cells were incubated in culture medium with 0.05% DMS0. To provide a control for PARP cleavage, C15 cells were treated for 12 h with the CD95 agonist antibody 7C11 (250 ng/ml) (Becton-Dickinson Biosciences, Le Pont de Claix, France). For toxicity assays, NPC cells were seeded in 96-well plastic microplates coated with polyHEMA at 75×10^3 cells/well in 150 μl of culture medium. Cell viability was evaluated using the WST-1 assay based on a soluble form of MTT [3-(4,5-dimethylthiazol-2-yl)2 2,5-diphenyl tetrazolium bromide] according to the manufacturer's instructions (Roche Molecular, Meylan, France). Cells were incubated with 10 μl of the WST-1 reagent added to the culture medium for 4 h at 37°C. The plates were subsequently read on an enzyme-linked immunosorbent assay reader (Dynatech MR7000) using a 450-nm filter. The mean and standard deviation were determined for quadruplicate samples.

RESULTS

Determination of optimal conditions for preparative immunoprecipitations of LMP1. We intended to identify novel proteins associated with LMP1 into lipid rafts derived from NPC cells including indirect partners and proteins whose expression was restricted to the NPC cell lineage. We chose a strategy based on preparative immunoprecipitation of LMP1-carrying complexes. Total raft complexes were isolated from C15 NPC tumor tissue by extraction in Triton lysis buffer and flotation on a density gradient. In the next step, LMP1-carrying complexes

TABLE 1. Examples of proteins identified by MS/MS following coimmunoprecipitation with the anti-LMP1 antibody OT21C applied on membrane rafts derived from the C15 NPC xenograft

Protein	Accession no.[a]	MW	Peptide no.	Peptide sequence(s)				
HSP90beta	NP_031381	83554	1	ADLINNLGTIAK				
HSP70 PROT5 (BiP)	NP_005338	72402	6	DAGTIAGLNVMR	TWNDPSVQQDIK	TFAPEEISAMVLTK	ITPSYVAFTPEGER	MKLSLVAAMLLLLSAAR
HSP70.1A	NP_005336	70280	6	DAGTIAGLNVLR	TTPSYVAFTDTER	AFYPEEISSMVLTK	IINEPTAAAIAYGLDR	NQVALNPQNTVFDAKR
Ribophorin 1	NP_002941	68641	5	FPLFGGWK	ALTSEIALLQSR	SEDLLDYGPFR	ATSFLLALEPELEAR	YDYQRQPDSGISSIR
Calnexin	NP_001737	67982	2	IVDDWANDGWGLKK	KIPNPDFFEDLEPFR			
TRAF3	Q13114	66015	2	NTGLLESQLSR	HIGDFKPDP			
Galectin-9	NP_033665	39835	3	FEDGGYVVCNTR	SILLSGTVLPSAQR	NTQIDNSWGSEER		

[a] NCBI RefSeq or Swiss.Prot database.

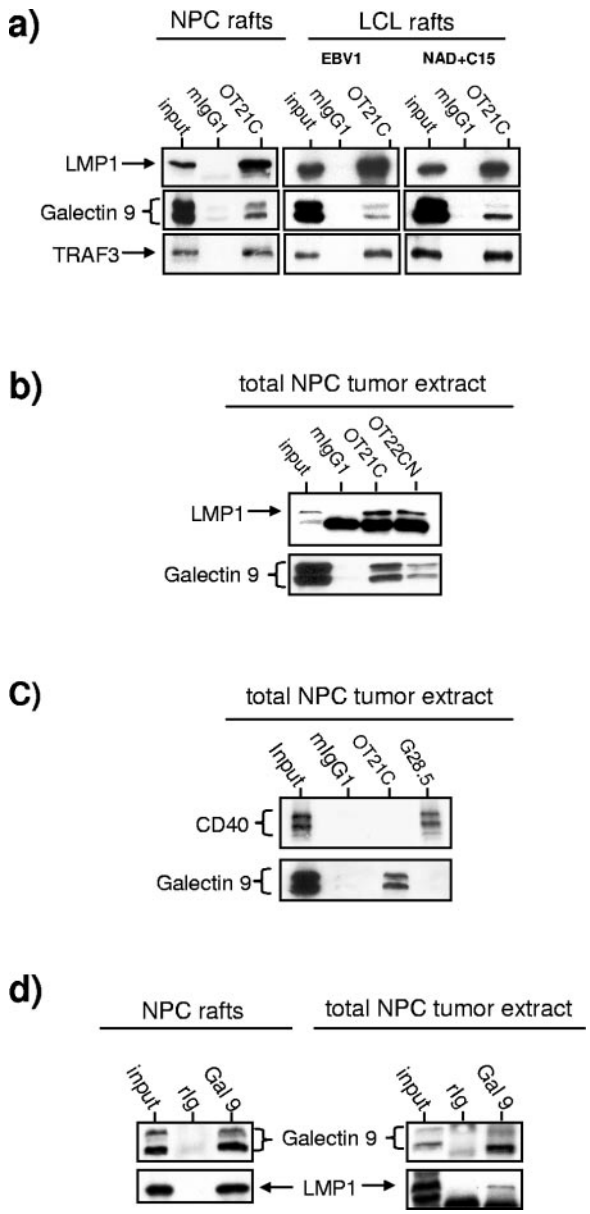

FIG. 2. Bidirectional coimmunoprecipitation of galectin 9 and LMP1 from NPC and LCL cell extracts. (a) Coimmunoprecipitation of galectin 9 and TRAF3 with the anti-LMP1 antibody OT21C reacting on NPC and LCL rafts. Raft samples (60 μg of protein) were prepared from the C15 NPC tumor line (NPC) and two EBV-transformed B-cell lines (EBV1 and NAD+C15) and submitted to analytical immunoprecipitation using 5 μg of purified IgG covalently bound to 5×10^7 magnetic beads. Precipitated proteins were analyzed in two parallel blots, one stained successively with anti-LMP1 (CS1-4) and anti-galectin 9 and the other stained with anti-TRAF3 antibodies. Input, 5 μg of raft-derived proteins saved prior to the immunoprecipitation step; mIgG1, control immunoprecipitation performed with mouse nonspecific IgG1; OT21C, LMP1 immunoprecipitation performed with OT21C (NPC, one-third of the eluted proteins; LCL, one-half of the eluted proteins). In the case of NAD+C15, there was a better recovery for the low-molecular-weight isoform of galectin 9. (b) Coimmunoprecipitation of galectin 9 with the anti-LMP1 OT21C and OT22CN antibodies reacting on whole-tumor extracts. Samples of C15 whole-tumor extracts (120 μg of protein) were submitted to immunoprecipitation using 5 μg of purified IgG coated on 5×10^7 magnetic beads (without covalent binding). Precipitated proteins were analyzed in successive Western blots stained with anti-LMP1 (CS1-4) and anti-galectin 9 antibodies. Because precipitating IgG was not covalently bound to magnetic beads, it was recovered in the eluate and stained on the Western membrane with the anti-mouse conjugate, just below the LMP1 band. Input, crude sample of C15 whole-tumor extract containing 30 μg of protein saved prior to the immunoprecipitation step; mIgG1, control immunoprecipitation; OT21C, LMP1 immunoprecipitation performed with the OT21C antibody directed to the large C-terminal intracytoplasmic region (residues 290 to 318) (one-half of the eluted proteins); OT22CN, LMP1 immunoprecipitation performed with the OT22CN antibody directed to the short N-terminal intracytoplasmic region (residues 1 to 23) (one-half of the eluted proteins). (c) Lack of coimmunoprecipitation of galectin 9 with an anti-CD40 antibody reacting on whole-tumor extracts. Samples of C15 whole-tumor extracts (120 μg of protein) were submitted to immunoprecipitation using 5 μg of purified IgG coated on 5×10^7 magnetic beads. Precipitated proteins were analyzed in parallel Western blots stained with anti-CD40 (MAb 89) and anti-galectin 9 antibodies. Protein gels prepared for CD40 detection were run in nondenaturing conditions as required for MAb 89 staining, thereby giving several bands and precluding molecular weight determination (8). Input, crude sample of C15 whole-tumor extract containing 40 μg of protein saved prior to the immunoprecipitation step; mIgG1, control immunoprecipitation; OT21C, LMP1 immunoprecipitation performed with the OT21C antibody (one-half of the eluted proteins); G28-5, CD40 immunoprecipitation performed with the G28-5 antibody (one-half of the eluted proteins). (d) Coimmunoprecipitation of LMP1 with an anti-galectin 9 antibody reacting on NPC rafts and whole-tumor extracts. C15 rafts (30 μg of protein) were submitted to immunoprecipitation using 2.5 μg of purified rabbit anti-galectin 9 Ig (loaded on 20 μl of protein A beads). Whole-tumor extracts (120 μg of protein) were treated with 3.75 μg of Ig loaded on 30 μl of beads. Precipitated proteins were analyzed in parallel Western blots stained with anti-galectin 9 (same rabbit polyclonal) and anti-LMP1 (CS1-4). Input, 10 μg of raft-derived protein or 30 μg of whole-tumor extract saved prior to the immunoprecipitation step; rIg, control immunoprecipitation performed with nonspecific rabbit Ig; gal9, galectin 9 immunoprecipitation performed with rabbit polyclonal antibodies directed to the C-terminal carbohydrate recognition domain of human galectin 9. This experiment was performed twice in duplicate. In each case, 25% and 100% of the eluted proteins were loaded in the gel for galectin 9 and LMP1 detection, respectively.

were captured using anti-LMP1 antibodies adsorbed on magnetic beads. This procedure was performed in experimental conditions compatible with preservation of raft lipid-protein interactions (1% Triton at 4°C in the absence of ionic detergents). During preliminary experiments OT21C was selected as the best precipitating antibody, being more efficient than S12 or OT22CN (data not shown). OT21C has been shown to bind a conformational epitope in the C-terminal intracytoplasmic region of LMP1 within residues 290 to 318 (44). Optimal ratios of antibody, magnetic beads, raft material, and reaction buffer volumes were determined in subsequent experiments. We found that it was possible to immunoprecipitate 100% LMP1 from a sample of C15 rafts corresponding to 60 μg of proteins, using 1.5×10^8 magnetic beads coated with 15 μg of affinity-purified OT21C, in a 600-μl reaction volume (Fig. 1). The same ratios of reagents and targets were used for subsequent preparative immunoprecipitations. In the same series of experiments, we were able to show that TRAF3 was coprecipitated with LMP1 but not the Lyn tyrosine-kinase, although it was abundant in the C15 raft fraction (Fig. 1). This was a good indication that we were able to perform selective capture of LMP1-carrying complexes from a composite mixture of membrane rafts.

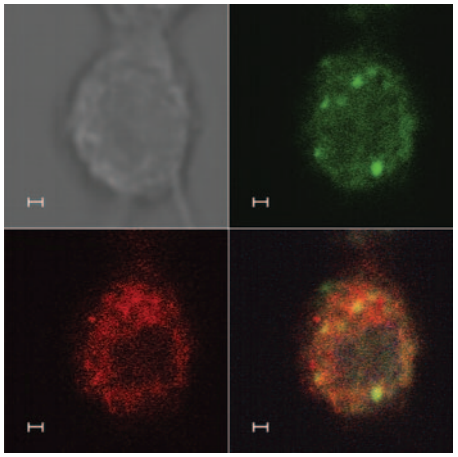

FIG. 3. Partial colocalization of LMP1 and galectin 9 in NPC cells. C15 NPC cells were double stained with a mouse anti-LMP1 (OT22CN; red secondary antibody, Alexa 546) (lower left) and a rabbit anti-Galectin 9 (green secondary antibody, Alexa 488) (upper right). Overlay (lower right). Scale bar, 1 μm. In this typical C15 cell, galectin 9 and LMP1 colocalize in dots where galectin 9 staining is prominent.

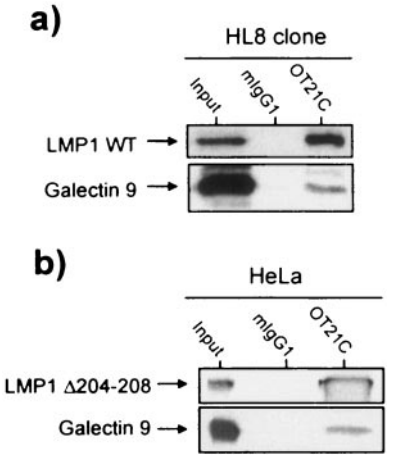

FIG. 4. LMP1-TRAF3 binding is not required for LMP1-galectin 9 interactions. (a) Coimmunoprecipitation of LMP1 and galectin 9 from rafts of HeLa cells stably transfected with the LMP1 gene (HL8 clone) and transiently transfected with the galectin 9 gene. (b) Coimmunoprecipitation of mutated LMP1 (deletion of the PXQXT motif at residues 204 to 208) and galectin 9 from rafts of transiently transfected HeLa cells. In both cases, raft samples (60 μg of protein) were treated with 5 μg of purified IgG coated on 0.5×10^8 magnetic beads (control IgG1 or OT21C). Precipitated proteins were analyzed in parallel Western blots stained with antibodies directed to LMP1 (CS1-4) and galectin 9 (rabbit polyclonal). WT, wild type.

Preparative immunoprecipitation of LMP1 and MS/MS identification of coimmunoprecipitated proteins. In the next step, we performed MS/MS analysis of the raft complexes immunoprecipitated from 180 μg of rafts using 4.5×10^8 magnetic beads coated with 45 μg of OT21C antibody. Two types of negative controls were used: C15 raft complexes submitted to immunoprecipitation with nonspecific IgG1 and complexes derived from the LMP1-negative C17 tumor line treated with OT21C. In order to reduce sample complexity, precipitated proteins eluted from the beads were submitted to a short migration (1 cm) on a small PAGE gel which was cut in nine slices. Proteins extracted from each slice were submitted to nano-liquid chromatography-electrospray ionization-quadryde time-of-flight analysis. This whole procedure was performed twice using either the C17/OT21C or the C15/IgG1 precipitates as controls. Proteins identified at least once in the C15/OT21C precipitate but not in the controls were retained as potential LMP1 partners (Table 1). TRAF3 was detected once in the OT21C precipitate whereas LMP1 itself was never detected, probably because it has only a few trypsin digestion sites (9 sites for LMP1 in contrast to 75 sites for TRAF3).

Demonstration of LMP1-galectin 9 interactions in NPC and LCL cells. Subsequent investigations were focused on galectin 9 for two main reasons: (i) this galactosyl binding protein is known to be very abundant in malignant cells of Hodgkin's disease, which is frequently associated with EBV and has intense LMP1 expression (21, 59); (ii) another human galectin, galectin 4, has been shown to play a role in the stability of lipid rafts (4, 22). A series of investigations was performed to confirm the interactions of LMP1 with galectin 9 using immunoprecipitation and Western blotting (Fig. 2). Galectin 9 was coprecipitated from NPC and LCL rafts by OT21C and revealed by using a specific polyclonal antibody. Depending on the experiment, two to four isoforms of galectin 9 were visualized in the crude raft extract as well as in the precipitate (Fig. 2a). These isoforms are generated by alternative splicing of exons 5 and 10, and possibly by posttranslational modifications (25, 41). Coprecipitation of galectin 9 was observed for both the EBV1 and NAD+C15 LCLs which carry the B95-8 and C15 strains of EBV, respectively. Galectin 9 was also coprecipitated from NPC whole-tumor extracts not only with the OT21C antibody (directed to the LMP1 C terminus) but also with OT22CN (directed to the LMP1 N terminus) (Fig. 2b). However, there was a higher relative amount of galectin 9 coprecipitated with OT21C (about 20% instead of 10% for OT22CN). To further assess the specificity of galectin 9 coprecipitation with LMP1, another type of control experiment was done using an antibody directed to the CD40 receptor, a cellular membrane protein which like LMP1 is constitutively accumulated in membrane rafts (2, 32). As shown in Fig. 2c, no galectin 9 was coimmunoprecipitated with CD40. The LMP1-galectin 9 interaction was also documented by doing coimmunoprecipitations of LMP1 with anti-galectin 9 antibodies. These experiments were performed on NPC rafts and whole-tumor extracts (Fig. 2d). Although the LMP1 band obtained from whole-tumor extract was faint, it was consistent in several experiments. Apparently, a smaller proportion of LMP1 molecules was coprecipitated with galectin 9 from whole-tumor extract compared to membrane rafts. One possible explanation could be that LMP1 and galectin 9 molecules interact more frequently in membrane rafts than in other cell compartments. To provide additional evidence of LMP1 interactions with galectin 9 at the single-cell level, we performed immunofluorescence staining of fixed cells and confocal analysis with anti-LMP1 and galectin 9 antibodies. Partial colocalization of these two proteins was observed in C15 NPC cells (Fig. 3).

TRAF3 binding to LMP1 is not required for LMP1-galectin 9 interactions. TRAF3 is a major partner protein of LMP1. We along with others have previously shown that it is recruited by

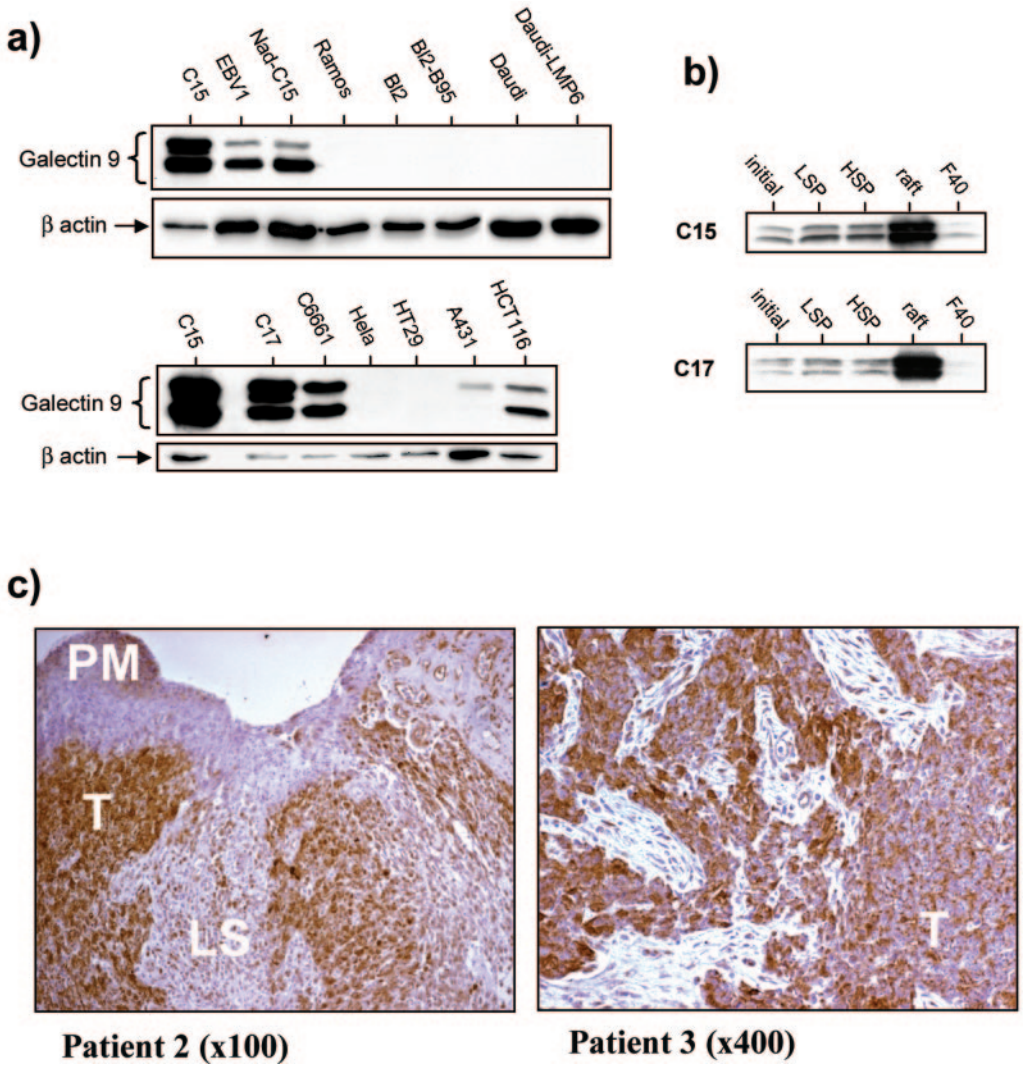

FIG. 5. Cell lineage and subcellular distribution of galectin 9. (a) Constitutive expression of galectin 9 in various types of lymphoid and epithelial cells. EBV1 and NAD+C15 are EBV-transformed B-cell lines (LCL). Ramos, BL2, and Daudi are Burkitt lymphoma cell lines. BL2-B95 was obtained by EBV conversion of BL2 cells infected with the B95-8 strain. Regarding epithelial cells, all protein extracts were prepared from xenografted tumors (C15 and C17 are permanently propagated into nude mice; other epithelial cells were specially grown as tumors into nude mice for the consistency of this analysis). For each cell type, 20 μg of whole-cell protein extract was analyzed by Western blotting. (b) Association of galectin 9 with membrane rafts in both LMP1-positive and -negative NPC cells. C15 and C17 tumor pieces were homogenized in MBS-Triton buffer, subjected to a raft flotation assay, and analyzed by Western blotting. The flotation assay generates three cell fractions in addition to the raft fraction: an LSP and an HSP, containing mostly cytoskeletal elements, and fraction F40 recovered in the 40% sucrose layer of the step gradient. F40 contains most components of the cytosol and nonraft membranes (11). Ten micrograms of protein was loaded per lane. In agreement with the data presented in panel a, galectin 9 was much more abundant in C15 than in C17 material (corresponding films were exposed 2 and 10 min, respectively). However, the ratio of galectin 9 concentration in the rafts compared to the initial extract was in the same range for the C15 (LMP1-positive) and the C17 (LMP1-negative) xenografts. (c) Galectin 9 expression in clinical specimens of NPC. NPC tissue sections from nine patients were stained with a primary anti-galectin 9 and a secondary peroxidase-labeled antibody and finally counterstained with Mayer's hematoxylin. Galectin 9 expression by malignant cells was found in all 9 biopsies; it was very intense for seven out of nine cases. Results from two patients (patients 2 and 3) are presented in this figure. A very strong expression of galectin 9 is visible in tumor cells (T). In contrast, galectin 9 is at a low abundance in the lymphoid stroma (LS) and the adjacent nonmalignant mucosa (PM; parakeratosic mucosa). In the case of patient 3, the staining of malignant cells is predominant at the plasma membrane.

LMP1 from the cytosol into membrane rafts (1, 2, 24). To determine whether TRAF3-LMP1 binding is required for LMP1 interaction with galectin 9, LMP1-galectin 9 association was investigated in HeLa cells transfected with the galectin 9 gene and either wild-type B95-8 LMP1 or a mutant LMP1 deleted of the critical TRAF3-binding motif PXQXT (residues 204 to 208) (45). As shown in Fig. 4, galectin 9 was coprecipitated with wild-type or mutant LMP1 with the same efficiency, providing evidence that TRAF3 is dispensable for galectin 9-LMP1 interaction. In addition, galectin 9 was also readily coprecipitated with another mutant form of LMP1 deleted not only of the PXQXT motif but also of the YDD motif (residues 384 to 386) which is required for LMP1-TRADD binding (data not shown) (37).

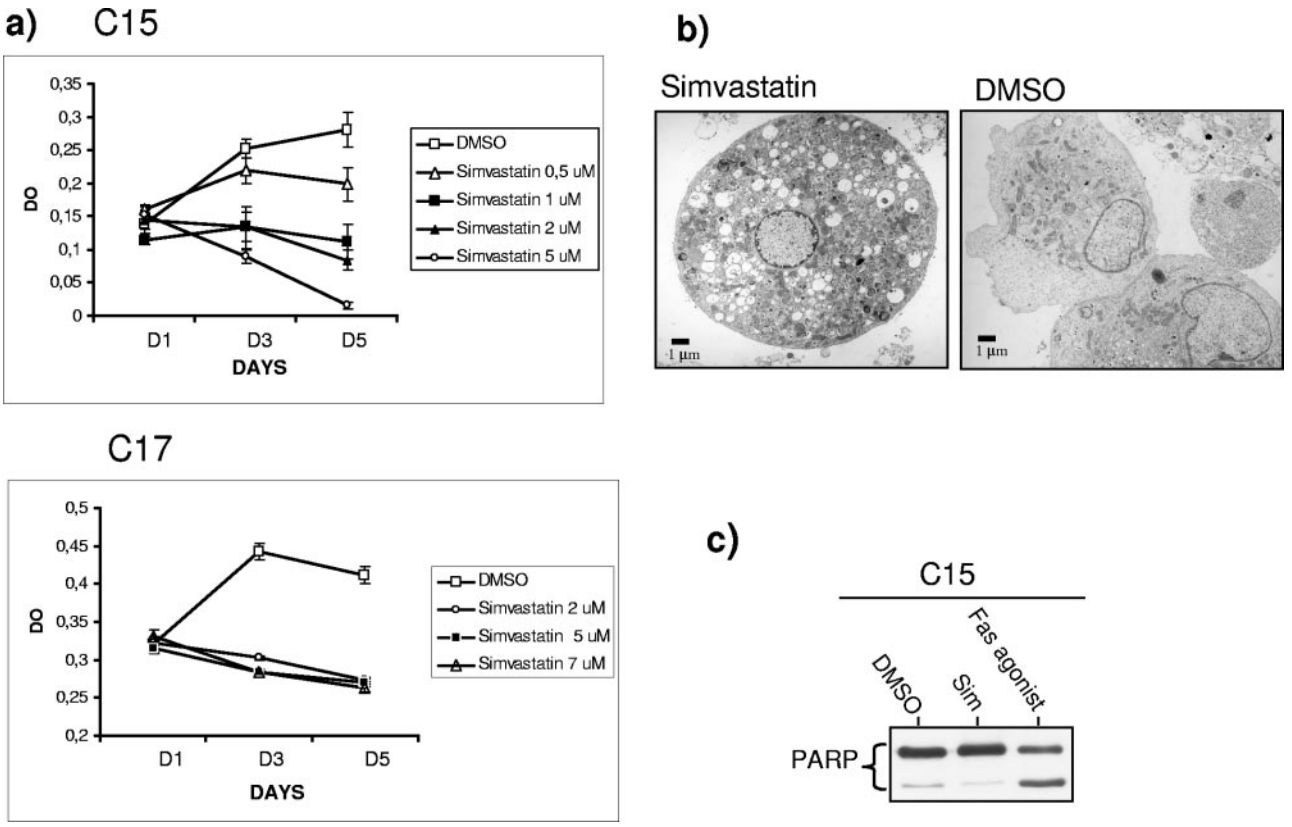

FIG. 6. Cytotoxic effects of Simvastatin on NPC cells. (a) C15 and C17 cells derived from xenografted tumors were short-term cultured for 5 days on a polyHEMA matrix in culture medium supplemented with vehicle (DMSO) only or various concentrations of Simvastatin. Cell viability was measured at days 1, 3, and 5 using a soluble form of MTT (see Materials and Methods). (b) Low-magnification electron micrographs showing one example of a C15 cell treated for 5 days with 5 μM Simvastatin and several control cells incubated with the vehicle (DMSO) by itself. Among the morphological changes induced by Simvastatin, note the loss of cellular connections, the transition to round-shaped cells and nuclei, the intense vacuolization, and the partial chromatin condensation at the periphery of the nucleus. (c) Assessment of PARP cleavage in C15 cells treated by Simvastatin (Sim) or the vehicle (DMSO) by itself. Thirty micrograms of protein derived from whole-cell extracts was loaded per lane. A positive control was provided by C15 cells treated with a Fas agonist for 12 h (7C11; 250 ng/ml); this sample contains the cleaved (89 kDa) in addition to the uncleaved (115 kDa) form of PARP.

Cell and tissue distribution of galectin 9. According to previous reports, galectin 9 expression is restricted to some normal tissues and some special types of malignancies (25). To obtain more information regarding the relationship between EBV infection and galectin 9 expression, we investigated its expression in a series of lymphoid and epithelial cells. Very intense expression was recorded in EBV-positive NPC tumor lines and EBV-transformed B-cell lines (EBV1 and NAD+ C15) (Fig. 5a). In contrast, all Burkitt cell lines were negative for galectin 9, including one originally infected by EBV (Daudi) and one converted by in vitro EBV infection (BL2-B95) (Fig. 5a). Although it was not as high as in C15, galectin 9 expression was very high in the LMP1-negative NPC tumor lines C17 and C666-1 (Fig. 5a). For both C15 and C17, there was a preferential association of galectin 9 with membrane rafts (Fig. 5b). In contrast, no galectin 9 expression or a much weaker expression was recorded in non-NPC EBV-negative epithelial cell lines (Fig. 5b). In summary, in vitro investigations suggested that a very high level of galectin 9 expression was a specific feature of NPC and LCL cells. To confirm galectin 9 expression by NPC cells in the patients, a series of fresh NPC biopsies was analyzed by immunohistochemistry with our anti-galectin 9 antibody. Intense galectin 9 expression by malignant cells was found in seven out of nine biopsies. Two characteristic examples are displayed in Fig. 5c. Two of nine specimens had weaker galectin 9 expression levels; they were peculiar, differentiated forms of NPC from French patients. Staining on infiltrating lymphocytes was much weaker in all specimens. Adjacent normal mucosa was either completely negative or weakly stained.

LMP1 and galectin 9 accumulation into NPC cell rafts is not inhibited by Simvastatin. It has been reported by Katano et al. that Simvastatin, an HMG (3-hydroxy-3-methylglutaryl)-coenzyme A reductase inhibitor and raft-modifying agent, induced dissociation of LMP1 from lipid rafts and subsequent apoptosis of LCL cells in about 5 days (31). Therefore, it was decided to assess the impact of Simvastatin on the raft distribution of LMP1 and galectin 9 in NPC cells. First, the range of active drug concentrations was determined in vitro on cells resulting from dispersion of the C15 and C17 xenografts using an assay of cell viability and proliferation. Significant decreases in cell viability were obtained when cells were treated for 5 days with concentrations of Simvastatin as low as 2 μM. These toxic effects were similar for the LMP1-positive and -negative NPC

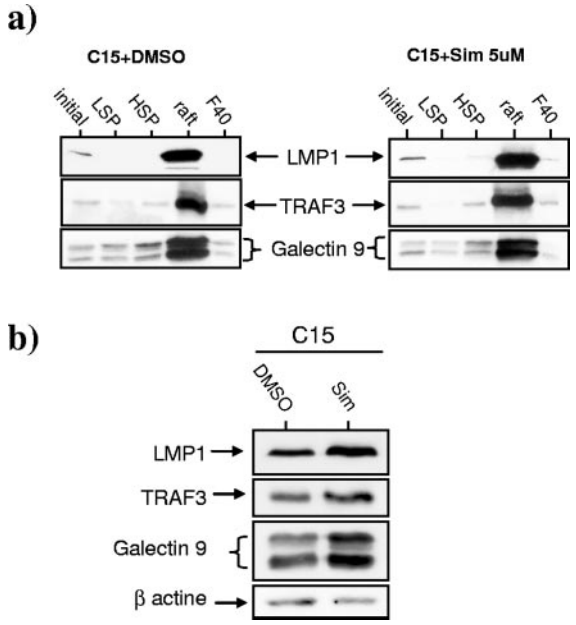

FIG. 7. Impact of Simvastatin on whole-cell concentration and raft distribution of LMP1, galectin 9, and TRAF3 in NPC cells. C15 cells derived from xenografted tumors were short-term cultured for 5 days on a polyHEMA matrix in the presence of 5 μM Simvastatin or DMSO alone and then subjected to protein extraction and a raft flotation assay. (a) Raft flotation assay of C15 cells treated by Simvastatin (Sim) or the vehicle (DMSO) by itself. The flotation assay generates three cell fractions in addition to the raft fraction: LSP and HSP containing mostly cytoskeletal elements and a fraction called F40 recovered in the 40% sucrose layer of the step gradient. F40 contains most components of the cytosol and nonraft membranes (11). Ten micrograms of proteins was loaded per lane. Parallel blots were done for detection of LMP1, TRAF3, and galectin 9. For all three proteins, the ratio of protein concentration in the rafts compared to the initial extract is not significantly different between Simvastatin-treated and control cells. (b) Comparison of whole-cell concentrations of LMP1, galectin 9, and TRAF3 in C15 cells treated for 5 days by Simvastatin (Sim) or the vehicle (DMSO) by itself (30 μg of protein per lane). An approximate twofold increase is observed in the whole-cell concentrations of LMP1 and galectin 9 in C15 cells treated by Simvastatin compared to the control.

cells derived from the C15 and C17 xenografts, respectively (Fig. 6a). C15 cells treated with 5 μM Simvastatin for 5 days were examined by electron microscopy. About 50% of treated cells displayed a morphology suggestive of necrosis (data not shown). Another subset of about 25% of cells underwent distinctive morphological changes: a general loss of cell connections, a transition to round-shaped cells and nuclei, and intense vacuolization (Fig. 6b). These alterations were reminiscent of morphological changes previously reported for pancreatic carcinoma cells treated with HMG-coenzyme A reductase inhibitors (38). In some cells, partial chromatin condensation at the periphery of the nucleus was suggestive of apoptosis-like programmed cell death, also called "caspase-independent apoptosis" (40) (Fig. 6b). Simvastatin did not stimulate PARP cleavage in C15 cells, providing additional evidence that drug toxicity was not mediated by massive caspase-dependent apoptosis (Fig. 6c). In subsequent experiments, raft distributions of LMP1, galectin 9, and TRAF3 were investigated in C15 cells treated with Simvastatin for 5 days. We could see no reduction in the amount of LMP1, TRAF3, and galectin 9 contained in C15 rafts using two concentrations of Simvastatin, i.e., 2 μM, which did not induce maximal toxicity (data not shown), and 5 μM (Fig. 7a). However, we noted a modest but consistent increase in the whole-cell concentration of LMP1 and galectin 9 (Fig. 7b).

DISCUSSION

The development of each type of EBV-associated malignancy requires a complex interplay between a specific cellular context and a specific mode of viral expression. Even in the restricted field of EBV-associated epithelial malignancies, there are major differences between EBV-associated gastric carcinomas and NPC in terms of cell differentiation and viral gene expression (56). Therefore, it is important to investigate the status of EBV products in cells that retain, as much as possible, the characteristics of NPC cells contained in clinical specimens. Such studies have long been hampered by technical difficulties in manipulating these cells in vitro. The development of proteomic methods has opened new possibilities. By application of preparative immunoprecipitation and mass spectrometry analysis on membrane rafts derived from an NPC xenograft, we have identified galectin 9 as a novel partner of LMP1. To our knowledge, it is the first example of a membrane protein that has been shown to specifically interact with LMP1. All previously described LMP1 partners are cytosolic molecules, for example, the TRAF molecules, TRADD, BRAM1, and SCF (Skp-cullin-F box) E3 ubiquitin ligase (10, 37, 58). We have found that galectin 9 is consistently and strongly expressed in NPC cells; in most cases, it is detected in malignant cells at a much higher level than in adjacent nonmalignant mucosa. Galectin 9 was first described in Hodgkin's disease as a tumor antigen (59). It has multiple functions including its role as a membrane urate transporter and eosinophil chemoattractant (25, 41, 42). It has a restricted tissue distribution. In mice, galectin 9 is strongly expressed by postnatal thymic epithelial cells and plays a role in clonal deletion of immature T cells (62). Interestingly, both the thymus epithelium and the nasopharyngeal mucosa derive from the embryonic pharyngeal endoderm (20). Galectin 9 is also expressed by LCL cells but not Burkitt lymphoma cells. In other words, all three types of EBV-transformed cells that have spontaneous LMP1 expression—Hodgkin cells, NPC, and LCL—also contain a high amount of galectin 9. However, it is obvious that, in terms of gene expression, galectin 9 expression is somehow independent of LMP1. For example, galectin 9 is readily detected in xenografted NPCs lacking LMP1-expression like C17 and C666-1. On the other hand, it does not show up in Burkitt cells converted by EBV or transfected with the LMP1 gene. In summary, galectin 9 expression in NPC seems to reflect a special mode of nasopharyngeal epithelial cell differentiation which is exacerbated in the context of cell transformation. Previous publications have shown that another human galectin, galectin 4, is accumulated in the rafts of intestinal epithelial cells, more precisely within a raft core component that is resistant to cholesterol extraction (4, 22). The latest of these reports provides evidence that galectin 4 plays a role in the stability of these structures (4). In light of our data, galectin 9

appears as one novel example of a galectin associated with membrane rafts.

The detection of large amounts of galectin 9 in NPC cells might also benefit our understanding of host-tumor interactions. NPCs are characterized by the presence of viral antigens in a highly inflammatory context, and the mechanisms of local immune tolerance are still poorly understood (3, 61). Therefore, it is noteworthy that galectin 9, like some other galectins, can act as a negative regulator of T-cell activation (30, 53). Because of its inhibitory effects on T cells, galectin 9 might possibly contribute to viral immune escape in NPC tumors. This hypothesis is supported by some of our recent experiments, which indicate that both LMP1 and galectin 9 can be released in the extracellular medium by NPC cells.

We have previously reported that LMP1 recruits its main adaptor TRAF3 in membrane rafts to the exclusion of TRAF2, TRAF1, or TRADD (1, 2). In contrast, galectin 9 is not recruited in membrane rafts by LMP1. It appears to be a resident raft protein even in the absence of LMP1, for example, in the C17 xenograft. In addition, it seems to be much more abundant than LMP1 in membrane rafts. According to preliminary experiments, the amount of LMP1 and galectin 9 molecules for 10 μg of rafts is about 200 and 1,200 fmol, respectively. This might explain the fact that it was difficult to precipitate more than 20% of the galectin 9 contained in the cellular extract even when it was possible to precipitate almost 100% of LMP1 (Fig. 2b). Using mutant forms of LMP1 expressed in HeLa cells, we have shown that its critical TRAF3- and TRADD-binding motifs are not required for its interaction with galectin 9. So far, we do not know whether LMP1 directly binds to galectin 9 or whether this interaction is mediated by other molecules, either lipids or proteins. Previous reports have shown that the short intracytoplasmic domain and a conserved motif of the first transmembrane segment are critical for LMP1 association with membrane rafts (12, 51, 65). Our ongoing experiments are intended to determine whether the same segments of LMP1 are required for its interaction with galectin 9.

Our data regarding LMP1-galectin 9 interactions provided a good molecular basis to investigate the effects of Simvastatin on the behavior of LMP1-carrying rafts in NPC cells. Treatment of C15 cells with Simvastatin was expected to induce the dissociation of LMP1 from membrane rafts, as previously reported for LCLs by Katano et al. (31). It was not the case: the raft distribution of LMP1 and TRAF3 as well as galectin 9 was apparently not affected by this drug, despite its strong cytotoxic effect. At the same time, the whole-cell concentrations of LMP1 and galectin 9 were increased under Simvastatin. Currently, we have no explanation for this modification. In any case, the cytotoxic effect of Simvastin against NPC cells was almost the same for C15 (LMP1-positive) and C17 (LMP1-negative) cells, providing additional evidence that LMP1 is not a critical lethal target for Simvastatin in this cell type. Interestingly, the cytotoxic effect of Simvastatin against NPC cells was obtained at low concentrations: a concentration of only 1 μM for 2 days was sufficient to induce significant growth inhibitory effects in contrast to a concentration of more than 10 μM required to achieve a significant effect on prostate carcinoma cells (67). Thus, our data suggest that Simvastatin might be beneficial in some circumstances for NPC patients. This is especially interesting since this drug has been widely used in medical practice for several years, allowing long-term monitoring of its undesirable effects.

ACKNOWLEDGMENTS

This work was supported by grants from the Ligue Nationale contre le Cancer (comité du Cher), from the Fondation de France (no. 2001004522), and from the ARC (no. 5238). C. K. was supported by a fellowship from the French Ministère de la Recherche et de la Technologie.

We thank V. Velasco for technical assistance and J. Wiels, M. Lipinski, and G. Pierron for helpful discussions.

REFERENCES

1. **Ardila-Osorio, H., B. Clausse, Z. Mishal, J. Wiels, T. Tursz, and P. Busson.** 1999. Evidence of LMP1-TRAF3 interactions in glycosphingolipid-rich complexes of lymphoblastoid and nasopharyngeal carcinoma cells. Int J. Cancer. **81:**645–649.
2. **Ardila-Osorio, H., C. Pioche-Durieu, F. Puvion-Dutilleul, B. Clausse, J. Wiels, W. Miller, N. Raab-Traub, and P. Busson.** 2005. TRAF interactions with raft-like buoyant complexes, better than TRAF rates of degradation, differentiate signaling by CD40 and EBV latent membrane protein 1. Int J. Cancer. **113:**267–275.
3. **Beck, A., D. Pazolt, G. G. Grabenbauer, J. M. Nicholls, H. Herbst, L. S. Young, and G. Niedobitek.** 2001. Expression of cytokine and chemokine genes in Epstein-Barr virus-associated nasopharyngeal carcinoma: comparison with Hodgkin's disease. J. Pathol. **194:**145–151.
4. **Braccia, A., M. Villani, L. Immerdal, L. L. Niels-Christiansen, B. T. Nystrom, G. H. Hansen, and E. M. Danielsen.** 2003. Microvillar membrane microdomains exist at physiological temperature. Role of galectin-4 as lipid raft stabilizer revealed by "superrafts." J. Biol. Chem. **278:**15679–15684.
5. **Brink, A. A., M. B. Vervoort, J. M. Middeldorp, C. J. Meijer, and A. J. van den Brule.** 1998. Nucleic acid sequence-based amplification, a new method for analysis of spliced and unspliced Epstein-Barr virus latent transcripts, and its comparison with reverse transcriptase PCR. J. Clin. Microbiol. **36:**3164–3169.
6. **Busson, P., G. Ganem, P. Flores, F. Mugneret, B. Clausse, B. Caillou, K. Braham, H. Wakasugi, M. Lipinski, and T. Tursz.** 1988. Establishment and characterization of three transplantable EBV-containing nasopharyngeal carcinomas. Int. J. Cancer. **42:**599–606.
7. **Busson, P., C. Keryer, T. Ooka, and M. Corbex.** 2004. EBV-associated nasopharyngeal carcinomas: from epidemiology to virus-targeting strategies. Trends Microbiol. **12:**356–360.
8. **Challa, A., M. H., M. Baker, J. Pound, J. Gordon.** 1997. CD40 workshop panel report, p. 159–161. *In* T. Kishimoto (ed.), Leucocyte typing. VI. White cell differentiation antigens, vol. 1. Garland Publishing, Inc., New York, N.Y.
9. **Cheung, S. T., D. P. Huang, A. B. Hui, K. W. Lo, C. W. Ko, Y. S. Tsang, N. Wong, B. M. Whitney, and J. C. Lee.** 1999. Nasopharyngeal carcinoma cell line (C666-1) consistently harbouring Epstein-Barr virus. Int. J. Cancer. **83:**121–126.
10. **Chung, P. J., Y. S. Chang, C. L. Liang, and C. L. Meng.** 2002. Negative regulation of Epstein-Barr virus latent membrane protein 1-mediated functions by the bone morphogenetic protein receptor IA-binding protein, BRAM1. J. Biol. Chem. **277:**39850–39857.
11. **Clausse, B., K. Fizazi, V. Walczak, C. Tetaud, J. Wiels, T. Tursz, and P. Busson.** 1997. High concentration of the EBV latent membrane protein 1 in glycosphingolipid-rich complexes from both epithelial and lymphoid cells. Virology **228:**285–293.
12. **Coffin, W. F., III, T. R. Geiger, and J. M. Martin.** 2003. Transmembrane domains 1 and 2 of the latent membrane protein 1 of Epstein-Barr virus contain a lipid raft targeting signal and play a critical role in cytostasis. J. Virol. **77:**3749–3758.
13. **Dawson, C. W., G. Tramountanis, A. G. Eliopoulos, and L. S. Young.** 2003. Epstein-Barr virus latent membrane protein 1 (LMP1) activates the phosphatidylinositol 3-kinase/Akt pathway to promote cell survival and induce actin filament remodeling. J. Biol. Chem. **278:**3694–3704.
14. **Devi, B. C., P. Pisani, T. S. Tang, and D. M. Parkin.** 2004. High incidence of nasopharyngeal carcinoma in native people of Sarawak, Borneo Island. Cancer Epidemiol. Biomarkers Prev. **13:**482–486.
15. **Dirmeier, U., R. Hoffmann, E. Kilger, U. Schultheiss, C. Briseno, O. Gires, A. Kieser, D. Eick, B. Sugden, and W. Hammerschmidt.** 2005. Latent membrane protein 1 of Epstein-Barr virus coordinately regulates proliferation with control of apoptosis. Oncogene **24:**1711–1717.
16. **Dolcetti, R., and J. Menezes.** 2003. Epstein-Barr virus and undifferentiated nasopharyngeal carcinoma: new immunobiological and molecular insights on a long-standing etiopathogenic association. Adv. Cancer Res. **87:**127–157.
17. **Edwards, R. H., D. Sitki-Green, D. T. Moore, and N. Raab-Traub.** 2004. Potential selection of LMP1 variants in nasopharyngeal carcinoma. J. Virol. **78:**868–881.
18. **Eliopoulos, A. G., E. R. Waites, S. M. Blake, C. Davies, P. Murray, and L. S. Young.** 2003. TRAF1 is a critical regulator of JNK signaling by the TRAF-

binding domain of the Epstein-Barr virus-encoded latent infection membrane protein 1 but not CD40. J. Virol. **77:**1316–1328.
19. **Gires, O., U. Zimber-Strobl, R. Gonnella, M. Ueffing, G. Marschall, R. Zeidler, D. Pich, and W. Hammerschmidt.** 1997. Latent membrane protein 1 of Epstein-Barr virus mimics a constitutively active receptor molecule. EMBO J. **16:**6131–6140.
20. **Gordon, J., V. A. Wilson, N. F. Blair, J. Sheridan, A. Farley, L. Wilson, N. R. Manley, and C. C. Blackburn.** 2004. Functional evidence for a single endodermal origin for the thymic epithelium. Nat. Immunol. **5:**546–553.
21. **Hammerschmidt, W., and B. Sugden.** 2004. Epstein-Barr virus sustains Burkitt's lymphomas and Hodgkin's disease. Trends Mol. Med. **10:**331–336.
22. **Hansen, G. H., L. Immerdal, E. Thorsen, L. L. Niels-Christiansen, B. T. Nystrom, E. J. Demant, and E. M. Danielsen.** 2001. Lipid rafts exist as stable cholesterol-independent microdomains in the brush border membrane of enterocytes. J. Biol. Chem. **276:**32338–32344.
23. **Heussinger, N., M. Buttner, G. Ott, E. Brachtel, B. Z. Pilch, E. Kremmer, and G. Niedobitek.** 2004. Expression of the Epstein-Barr virus (EBV)-encoded latent membrane protein 2A (LMP2A) in EBV-associated nasopharyngeal carcinoma. J. Pathol. **203:**696–699.
24. **Higuchi, M., K. M. Izumi, and E. Kieff.** 2001. Epstein-Barr virus latent-infection membrane proteins are palmitoylated and raft-associated: protein 1 binds to the cytoskeleton through TNF receptor cytoplasmic factors. Proc. Natl. Acad. Sci. USA **98:**4675–4680.
25. **Hirashima, M., Y. Kashio, N. Nishi, A. Yamauchi, T. A. Imaizumi, T. Kageshita, N. Saita, and T. Nakamura.** 2004. Galectin-9 in physiological and pathological conditions. Glycoconj. J. **19:**593–600.
26. **Huang, Y. T., T. S. Sheen, C. L. Chen, J. Lu, Y. Chang, J. Y. Chen, and C. H. Tsai.** 1999. Profile of cytokine expression in nasopharyngeal carcinomas: a distinct expression of interleukin 1 in tumor and CD4+ T cells. Cancer Res. **59:**1599–1605.
27. **Huen, D. S., S. A. Henderson, D. Croom-Carter, and M. Rowe.** 1995. The Epstein-Barr virus latent membrane protein-1 (LMP1) mediates activation of NF-kappa B and cell surface phenotype via two effector regions in its carboxy-terminal cytoplasmic domain. Oncogene **10:**549–560.
28. **Iwakiri, D., T. S. Sheen, J. Y. Chen, D. P. Huang, and K. Takada.** 2005. Epstein-Barr virus-encoded small RNA induces insulin-like growth factor 1 and supports growth of nasopharyngeal carcinoma-derived cell lines. Oncogene **24:**1767–1773.
29. **Izumi, K. M., K. M. Kaye, and E. D. Kieff.** 1994. Epstein-Barr virus recombinant molecular genetic analysis of the LMP1 amino-terminal cytoplasmic domain reveals a probable structural role, with no component essential for primary B-lymphocyte growth transformation. J. Virol. **68:**4369–4376.
30. **Kashio, Y., K. Nakamura, M. J. Abedin, M. Seki, N. Nishi, N. Yoshida, T. Nakamura, and M. Hirashima.** 2003. Galectin-9 induces apoptosis through the calcium-calpain-caspase-1 pathway. J. Immunol. **170:**3631–3636.
31. **Katano, H., L. Pesnicak, and J. I. Cohen.** 2004. Simvastatin induces apoptosis of Epstein-Barr virus (EBV)-transformed lymphoblastoid cell lines and delays development of EBV lymphomas. Proc. Natl. Acad. Sci. USA **101:**4960–4965.
32. **Kaykas, A., K. Worringer, and B. Sugden.** 2001. CD40 and LMP-1 both signal from lipid rafts but LMP-1 assembles a distinct, more efficient signaling complex. EMBO J. **20:**2641–2654.
33. **Kaykas, A., K. Worringer, and B. Sugden.** 2002. LMP-1's transmembrane domains encode multiple functions required for LMP-1's efficient signaling. J. Virol. **76:**11551–11560.
34. **Kennedy, G., J. Komano, and B. Sugden.** 2003. Epstein-Barr virus provides a survival factor to Burkitt's lymphomas. Proc. Natl. Acad. Sci. USA **100:**14269–14274.
35. **Khabir, A., A. Ghorbel, J. Daoud, M. Frikha, M. M. Drira, A. Laplanche, P. Busson, and R. Jlidi.** 2003. Similar BCL-X but different BCL-2 levels in the two age groups of North African nasopharyngeal carcinomas. Cancer Detect. Prev. **27:**250–255.
36. **Khabir, A., H. Karray, S. Rodriguez, M. Rosé, J. Daoud, M. Frikha, T. Boudawara, J. Middeldorp, R. Jlidi, and P. Busson.** 2005. EBV latent membrane protein 1 abundance correlates with patient age but not with metastatic behavior in North-African nasopharyngeal carcinomas. Virol. J. **2:**39.
37. **Kieser, A., C. Kaiser, and W. Hammerschmidt.** 1999. LMP1 signal transduction differs substantially from TNF receptor 1 signaling in the molecular functions of TRADD and TRAF2. EMBO J. **18:**2511–2521.
38. **Kusama, T., M. Mukai, T. Iwasaki, M. Tatsuta, Y. Matsumoto, H. Akedo, and H. Nakamura.** 2001. Inhibition of epidermal growth factor-induced RhoA translocation and invasion of human pancreatic cancer cells by 3-hydroxy-3-methylglutaryl-coenzyme A reductase inhibitors. Cancer Res. **61:**4885–4891.
39. **Lam, N., M. L. Sandberg, and B. Sugden.** 2004. High physiological levels of LMP1 result in phosphorylation of eIF2α in Epstein-Barr virus-infected cells. J. Virol. **78:**1657–1664.
40. **Leist, M., and M. Jaattela.** 2001. Four deaths and a funeral: from caspases to alternative mechanisms. Nat. Rev. Mol. Cell Biol. **2:**589–598.
41. **Lipkowitz, M. S., E. Leal-Pinto, B. E. Cohen, and R. G. Abramson.** 2004. Galectin 9 is the sugar-regulated urate transporter/channel UAT. Glycoconj. J. **19:**491–498.
42. **Liu, F. T., and G. A. Rabinovich.** 2005. Galectins as modulators of tumour progression. Nat. Rev. Cancer **5:**29–41.
43. **Luftig, M., E. Prinarakis, T. Yasui, T. Tsichritzis, E. Cahir-McFarland, J. Inoue, H. Nakano, T. W. Mak, W. C. Yeh, X. Li, S. Akira, N. Suzuki, S. Suzuki, G. Mosialos, and E. Kieff.** 2003. Epstein-Barr virus latent membrane protein 1 activation of NF-kappaB through IRAK1 and TRAF6. Proc. Natl. Acad. Sci. USA **100:**15595–15600.
44. **Meij, P., M. B. Vervoort, J. Aarbiou, P. van Dissel, A. Brink, E. Bloemena, C. J. Meijer, and J. M. Middeldorp.** 1999. Restricted low-level human antibody responses against Epstein-Barr virus (EBV)-encoded latent membrane protein 1 in a subgroup of patients with EBV-associated diseases. J. Infect. Dis. **179:**1108–1115.
45. **Miller, W. E., J. L. Cheshire, A. S. Baldwin, Jr., and N. Raab-Traub.** 1998. The NPC derived C15 LMP1 protein confers enhanced activation of NF-kappa B and induction of the EGFR in epithelial cells. Oncogene **16:**1869–1877.
46. **Miller, W. E., J. L. Cheshire, and N. Raab-Traub.** 1998. Interaction of tumor necrosis factor receptor-associated factor signaling proteins with the latent membrane protein 1 PXQXT motif is essential for induction of epidermal growth factor receptor expression. Mol. Cell. Biol. **18:**2835–2844.
47. **Nicholls, J. M., A. Agathanggelou, K. Fung, X. Zeng, and G. Niedobitek.** 1997. The association of squamous cell carcinomas of the nasopharynx with Epstein-Barr virus shows geographical variation reminiscent of Burkitt's lymphoma. J. Pathol. **183:**164–168.
48. **Pike, L. J.** 2004. Lipid rafts: heterogeneity on the high seas. Biochem. J. **378:**281–292.
49. **Puls, A., A. G. Eliopoulos, C. D. Nobes, T. Bridges, L. S. Young, and A. Hall.** 1999. Activation of the small GTPase Cdc42 by the inflammatory cytokines TNFα and IL-1, and by the Epstein-Barr virus transforming protein LMP1. J. Cell Sci. **112:**2983–2992.
50. **Raab-Traub, N.** 2002. Epstein-Barr virus in the pathogenesis of NPC. Semin. Cancer Biol. **12:**431–441.
51. **Rothenberger, S., M. Rousseaux, H. Knecht, F. C. Bender, D. F. Legler, and C. Bron.** 2002. Association of the Epstein-Barr virus latent membrane protein 1 with lipid rafts is mediated through its N-terminal region. Cell Mol. Life Sci. **59:**171–180.
52. **Rowe, M., H. S. Evans, L. S. Young, K. Hennessy, E. Kieff, and A. B. Rickinson.** 1987. Monoclonal antibodies to the latent membrane protein of Epstein-Barr virus reveal heterogeneity of the protein and inducible expression in virus-transformed cells. J. Gen. Virol. **68:**1575–1586.
53. **Rubinstein, N., M. Alvarez, N. W. Zwirner, M. A. Toscano, J. M. Ilarregui, A. Bravo, J. Mordoh, L. Fainboim, O. L. Podhajcer, and G. A. Rabinovich.** 2004. Targeted inhibition of galectin-1 gene expression in tumor cells results in heightened T cell-mediated rejection. A potential mechanism of tumor-immune privilege. Cancer Cell **5:**241–251.
54. **Sbih-Lammali, F., B. Clausse, H. Ardila-Osorio, R. Guerry, M. Talbot, S. Havouis, L. Ferradini, J. Bosq, T. Tursz, and P. Busson.** 1999. Control of apoptosis in Epstein-Barr virus-positive nasopharyngeal carcinoma cells: opposite effects of CD95 and CD40 stimulation. Cancer Res. **59:**924–930.
55. **Seto, E., L. Yang, J. Middeldorp, T. S. Sheen, J. Y. Chen, M. Fukayama, Y. Eizuru, T. Ooka, and K. Takada.** 2005. Epstein-Barr virus (EBV)-encoded BARF1 gene is expressed in nasopharyngeal carcinoma and EBV-associated gastric carcinoma tissues in the absence of lytic gene expression. J. Med. Virol. **76:**82–88.
56. **Takada, K.** 2000. Epstein-Barr virus and gastric carcinoma. Mol. Pathol. **53:**255–261.
57. **Tang, K. F., S. Y. Tan, S. H. Chan, S. M. Chong, K. S. Loh, L. K. Tan, and H. Hu.** 2001. A distinct expression of CC chemokines by macrophages in nasopharyngeal carcinoma: implication for the intense tumor infiltration by T lymphocytes and macrophages. Hum. Pathol. **32:**42–49.
58. **Tang, W., O. A. Pavlish, V. S. Spiegelman, A. A. Parkhitko, and S. Y. Fuchs.** 2003. Interaction of Epstein-Barr virus latent membrane protein 1 with SCFHOS/beta-TrCP E3 ubiquitin ligase regulates extent of NF-kappaB activation. J. Biol. Chem. **278:**48942–48949.
59. **Tureci, O., H. Schmitt, N. Fadle, M. Pfreundschuh, and U. Sahin.** 1997. Molecular definition of a novel human galectin which is immunogenic in patients with Hodgkin's disease. J. Biol. Chem. **272:**6416–6422.
60. **Vicat, J. M., H. Ardila-Osorio, A. Khabir, M. C. Brezak, I. Viossat, P. Kasprzyk, R. Jlidi, P. Opolon, T. Ooka, G. Prevost, D. P. Huang, and P. Busson.** 2003. Apoptosis and TRAF-1 cleavage in Epstein-Barr virus-positive nasopharyngeal carcinoma cells treated with doxorubicin combined with a farnesyl-transferase inhibitor. Biochem. Pharmacol. **65:**423–433.
61. **Voo, K. S., T. Fu, H. Y. Wang, J. Tellam, H. E. Heslop, M. K. Brenner, C. M. Rooney, and R. F. Wang.** 2004. Evidence for the presentation of major histocompatibility complex class I-restricted Epstein-Barr virus nuclear antigen 1 peptides to CD8+ T lymphocytes. J. Exp. Med. **199:**459–470.
62. **Wada, J., K. Ota, A. Kumar, E. I. Wallner, and Y. S. Kanwar.** 1997. Developmental regulation, expression, and apoptotic potential of galectin-9, a beta-galactoside binding lectin. J. Clin. Investig. **99:**2452–2461.
63. **Wang, F., C. Gregory, C. Sample, M. Rowe, D. Liebowitz, R. Murray, A. Rickinson, and E. Kieff.** 1990. Epstein-Barr virus latent membrane protein (LMP1) and nuclear proteins 2 and 3C are effectors of phenotypic changes

in B lymphocytes: EBNA-2 and LMP1 cooperatively induce CD23. J. Virol. **64:**2309–2318.
64. **Xie, P., B. S. Hostager, and G. A. Bishop.** 2004. Requirement for TRAF3 in signaling by LMP1 but not CD40 in B lymphocytes. J. Exp. Med. **199:**661–671.
65. **Yasui, T., M. Luftig, V. Soni, and E. Kieff.** 2004. Latent infection membrane protein transmembrane FWLY is critical for intermolecular interaction, raft localization, and signaling. Proc. Natl. Acad. Sci. USA **101:**278–283.
66. **Zhang, X., W. Uthaisang, L. Hu, I. T. Ernberg, and B. Fadeel.** 2005. Epstein-Barr virus-encoded latent membrane protein 1 promotes stress-induced apoptosis upstream of caspase-2-dependent mitochondrial perturbation. Int. J. Cancer. **113:**397–405.
67. **Zhuang, L., J. Kim, R. M. Adam, K. R. Solomon, and M. R. Freeman.** 2005. Cholesterol targeting alters lipid raft composition and cell survival in prostate cancer cells and xenografts. J. Clin. Investig. **115:**959–968.